Cooperative Control Strategy of Energy Storage System and Microsources for Stabilizing the Microgrid during Islanded Operation

Jong-Yul Kim, *Member, IEEE*, Jin-Hong Jeon, *Member, IEEE*, Seul-Ki Kim, *Member, IEEE*, Changhee Cho, *Member, IEEE*, June Ho Park, Hak-Man Kim, *Member, IEEE*, and Kee-Young Nam

***Abstract*—In this paper, the cooperative control strategy of microsources and the energy storage system (ESS) during islanded operation is presented and evaluated by a simulation and experiment. The ESS handles the frequency and the voltage as a primary control. And then, the secondary control in microgrid management system returns the current power output of the ESS into zero. The test results show that the proposed cooperative control strategy can regulate the frequency and the voltage, and the secondary control action can contribute to improve the control capability.**

***Index Terms*—Cooperative control, energy storage system (ESS), islanded operation, microgrid, microgrid management system (MMS).**

I. Introduction

THOUGH the penetration of distributed generations (DGs) to the electric power system is limited due to the lack of economical benefits, it will be accelerated for various reasons. The increase in DGs penetration depth and the presence of multiple DGs in electrical proximity to one another have brought about the concept of the microgrid [1]–[4], which is a cluster of interconnected DGs, loads, and intermediate energy storage systems (ESSs). Compared to a single DG, the microgrid can provide more technical benefits and control flexibilities to utility grid. The microgrid also offers economical opportunities through introducing the combined heat and power (CHP) units, which is currently the most important means of improving energy efficiency [5], [6]. The microgrid can operate both in grid connect and in islanded operation mode [7]. The balance between supply and demand of power is one of the most important requirements of microgrid management. In the grid-interconnected mode, the microgrid exchanges power to an interconnected grid to meet the balance. On the other hand, in the islanded mode, the microgrid should meet the balance using the decrease in generation or load shedding. Many related technologies on islanded operation of microgrid such as management, control, protection, power quality, pilot plants, and field tests have been studied. Energy management and power control for microgrid have been studied [8]–[18]. Protection schemes for microgrid during voltage sags have been developed and tested using an emulated laboratory microgrid system [19], [20]. Development of pilot plants for microgrid and field tests have been performed for frequency- and voltage-control algorithms, and for utility interconnection devices [2], [21]–[23]. As usual, the microgrid operates in grid-connect mode, but, when a fault occurs in the upstream grid, it should disconnect and shift into islanded operation mode. In grid-connect mode, the frequency and the voltage of the microgrid are maintained within a tight range by the main grid. In an islanded operation, however, which has relatively few microsources, the local frequency and the voltage control of the microgrid is not straightforward. During islanding, the power balance between supply and demand does not match at the moment. As a result, the frequency and the voltage of the microgrid will fluctuate, and the system can experience a blackout unless there is an adequate power-balance matching process. A microgrid composed only of renewable energy sources (RESs) and conventional CHP units, such as the diesel generator, gas engine, and microturbine is hard to make sure the good dynamic performance of microgrid during islanded operation due to the intrinsic characteristics of these generation systems. The RES has an intermittent nature since their power outputs depend on the availability of the primary source, wind, sun, etc., and therefore, they cannot guarantee by themselves the power supply required by loads. On the other hand, CHP systems are limited by their insufficient dynamic performance for load tracking [24], [25]. Especially, the frequency of the microgrid may change rapidly due to the low inertia present in the microgrid. Therefore, local frequency control is one of the main issues in islanded operation [26]. To overcome these limitations, the introduction of the ESS is considered as an effective solution. The ESS is based on power electronic device and has a very fast response time. Therefore, a properly designed ESS can allow a system to stabilize by absorbing and injecting instantaneous power. There are some previous studies on the application of the ESS for stabilizing the power systems and the RES. In [27]–[29], a control scheme for reducing a power fluctuation of wind-generation system is presented. This scheme utilizes the stored energy of the ESS to

Manuscript received July 1, 2010; revised August 16, 2010; accepted August 17, 2010. Date of current version December 27, 2010. Recommended for publication by Associate Editor J. M. Guerrero.

J.-Y. Kim, J.-H. Jeon, S.-K. Kim, and C. Cho are with the New & Renewable Energy System Research Center, Korea Electrotechnology Research Institute, Changwon 641-120, Korea (e-mail: jykim@keri.re.kr; jhjeon@keri.re.kr; blksheep@keri.re.kr; chcho@keri.re.kr).

J. H. Park is with the Department of Electrical Engineering, Pusan National University, Busan 609-735, Korea (e-mail: parkjh@pusan.ac.kr).

H.-M. Kim is with the Department of Electrical Engineering, University of Incheon, Incheon 406-772, Korea (e-mail: hmkim@incheon.ac.kr).

K.-Y. Nam is with the Research and Development Center, Halla Energy & Environment, Seoul 138-811, Korea (e-mail: kynam@hallasanup.com).

Color versions of one or more of the figures in this paper are available online at http://ieeexplore.ieee.org.

Digital Object Identifier 10.1109/TPEL.2010.2073488

smoothen the power output of wind-generation system. In addition, the ESS can contribute to stabilize the frequency of large bulk power system. In [30]–[32], fast-acting ESSs can effectively damp electromechanical oscillations in a power system, because they provide storage capacity in addition to the kinetic energy of the generator rotors, which can share sudden changes in power requirement. The discussion of introducing the ESS in microgrid is presented in [33]–[37]. The power-electronics-interfaced DG system with the ESS is presented in [33]–[35]. The DG system comprises a primary energy source ESS and an inverter. The ESS is installed in common dc link to complement the slower power output of primary energy source, particularly fuel cell. Through installing the ESS into DG system with relatively slow response primary energy source, the microgrid can operate in a stable way during islanded mode even though the load is changed in a sudden. The application of electric double-layer capacitor (EDLC) as a power system stabilizer is presented in [36]. In this work, the control method of EDLC is proposed to maintain the power quality of microgrid in islanded operation. From the previous works, the cooperative control scheme between the ESS and other microsources is needed to effectively achieve the goal in islanded operation. The control concept, which consists of primary and secondary control is proposed to stabilize the frequency of microgrid [37]. This concept mimics the frequency control way of the bulk power system [38]. The ESS absorbs or injects the power through the droop characteristic and the frequency deviation is removed by automatic generation control (AGC) of supervisory controller. This paper addresses the cooperative control strategy of microgrid for islanded operation not only for the frequency, but also for the voltage. In this control scheme, two layered cooperative control structure is applied: the primary control action in the ESS and the secondary control action in the microgrid management system (MMS). The constant frequency and constant voltage (CFCV) control method of the ESS is applied by primary control, and the secondary control of MMS regulates the power output of the ESS to be zero. To evaluate the proposed strategy, a test system is defined and dynamic simulation model based on PSCAD/EMTDC is developed. In addition, a 120-kW microgrid pilot plant and its supervisory control system (MMS) were developed. The simulation and experimental results were presented and discussed to evaluate the dynamic performance of the proposed control strategy for islanded operation. Section II of the paper introduces the background of microgrid. Section III discusses the configuration of test system and Section IV describes the proposed control strategy of microgrid. Results of the study and discussions are reported in Sections V and VI, respectively. Conclusion is stated in Section VII.

II. Background

A. Microgrid

Fig. 1 shows a typical configuration of a microgrid. It comprises, in addition to loads, RES as well as a diesel engine, gas engine, micro turbine, and an ESS as support systems to fulfill the stable operation of a facility. This microgrid is connected to the grid at the point of common coupling (PCC), and operates in parallel with a utility grid under normal situations. The microgrid disconnects from the utility grid, however, and transfers into islanded operation mode when a fault occurs in the upstream grid. The intermediate ESS is an inverter-interfaced battery bank [(battery energy storage system (BESS)], superconducting magnetic energy storage (SMES), super capacitor or flywheel. The storage device in the microgrid is analogous to the spinning reserve of large generators in the conventional grid. They ensure the balance between energy generation and consumption especially during islanded operation [39].

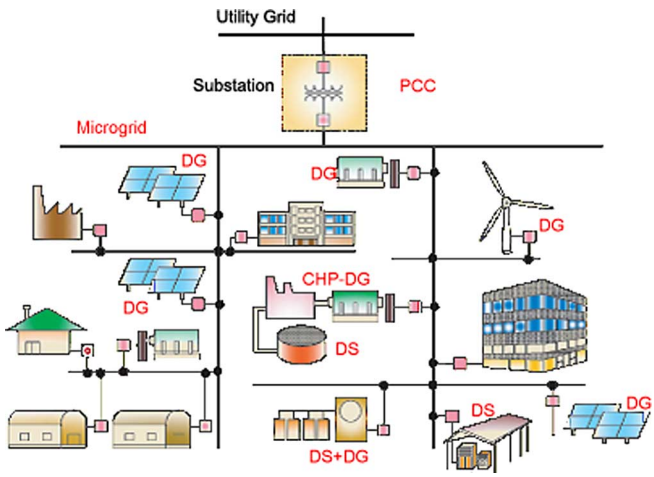

Fig. 1. Typical configuration of a microgrid [40].

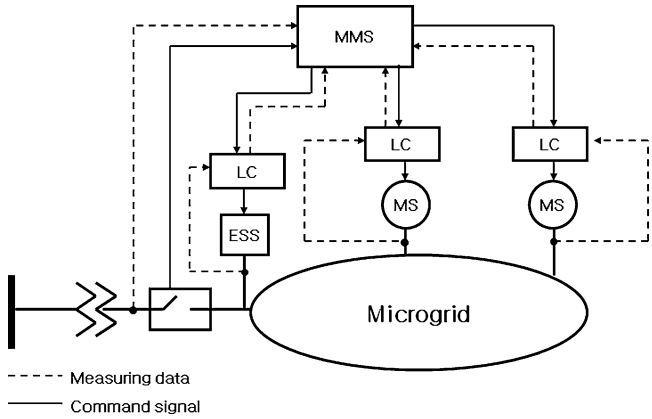

Fig. 2. Hierarchical control structure of microgrid.

B. Hierarchical Control Structure of Microgrid

The microgrid has a hierarchical control structure, as shown in Fig. 2. It has two control layers: MMS and local controller (LC). The MMS is a centralized controller that deals with management functions, such as disconnection and resynchronization of the microgrid and the load-shedding process. In addition to this function, the MMS is responsible for the supervisory control of microsources and the ESS. Using collected local information, the MMS generates a power output set point and provides it to the LCs. An LC is a local controller that is located at each microsource and controls the power output according to the power output set point from the MMS [37].

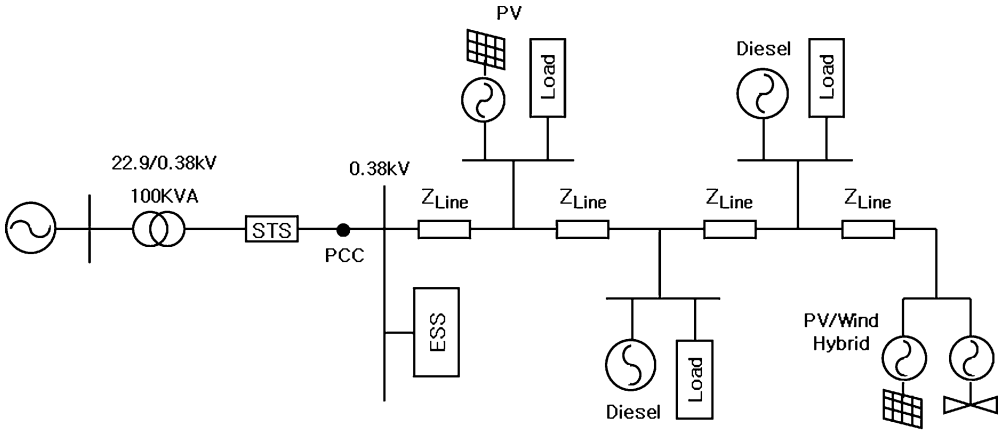

Fig. 3. Configuration of the studied microgrid.

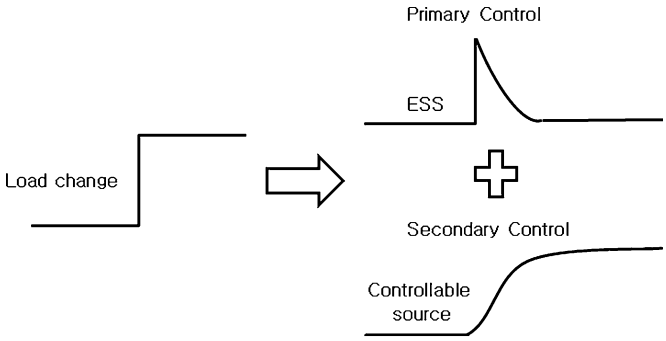

Fig. 4. Concept of control strategy for islanded operation.

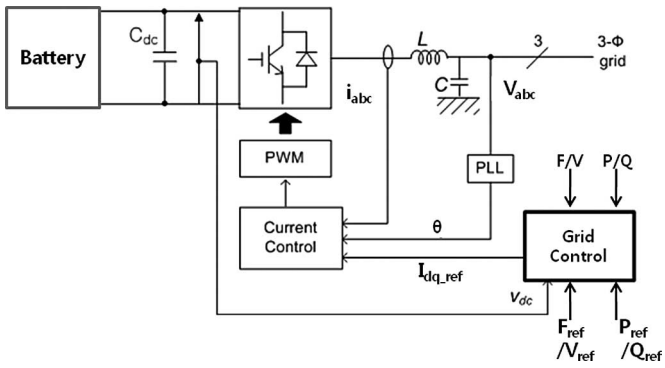

Fig. 5. Configuration of the BESS.

III. Study System Configuration

Fig. 3 presents the configuration of the studied microgrid pilot plant system, which has been constructed in Korea Electrotechnology Research Institute. The microgrid system is composed of a 380-V, one-feeder distribution subsystem, which is connected to a 22.9-kV distribution network through a 100-kVA pole transformer.

The system includes a photovoltaic (PV), PV and WT hybrid system (H/B) (PV and wind turbine (WT) hybrid) system, two diesel generators, BESS, static transfer switch (STS), and three loads. These components have been connected to 380-V low voltage lines, which connects to a 380-V busbar. The 10-kW PV system is not a real PV generation system but a simulator that

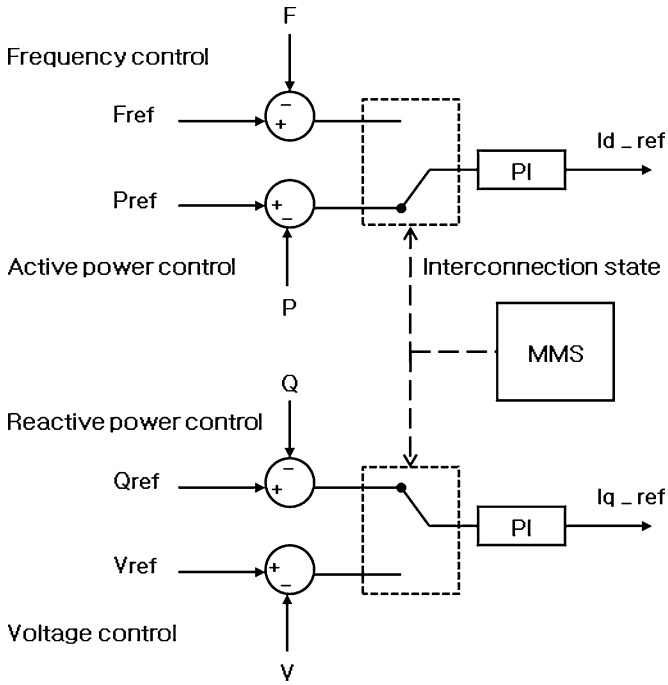

Fig. 6. Block diagram of grid controller.

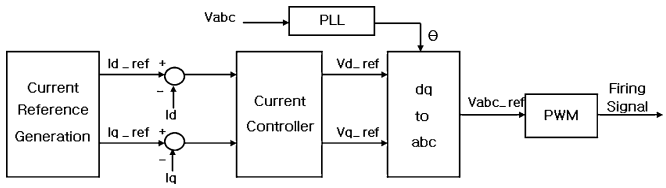

Fig. 7. Current control scheme of the ESS.

mimics the real PV generation system. The 20-kW hybrid system is composed of a wind turbine simulator (10 kW), a real PV array (10 kW), a common dc bus, and a grid-interface inverter (20 kW). The BESS is connected to 380-V busbar, which is near the PCC to be utilized when the system transit to the islanded operation mode. The system also includes two diesel generators, i.e., 50-kW and 20-kW diesel generators on the feeder. The STS is also connected to 380-V busbar to disconnect microgrid from

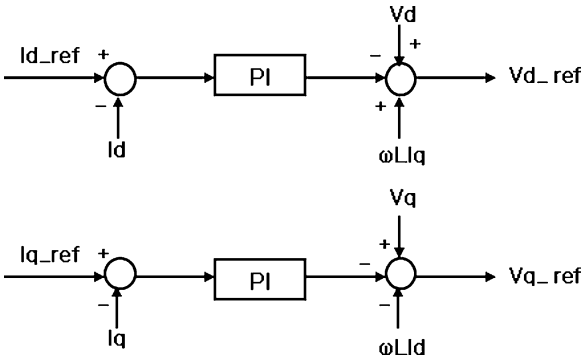

Fig. 8. Block diagram of current controller.

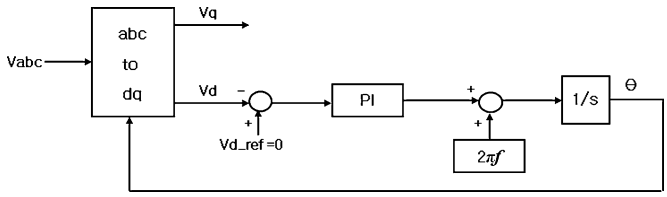

Fig. 9. Block diagram of PLL.

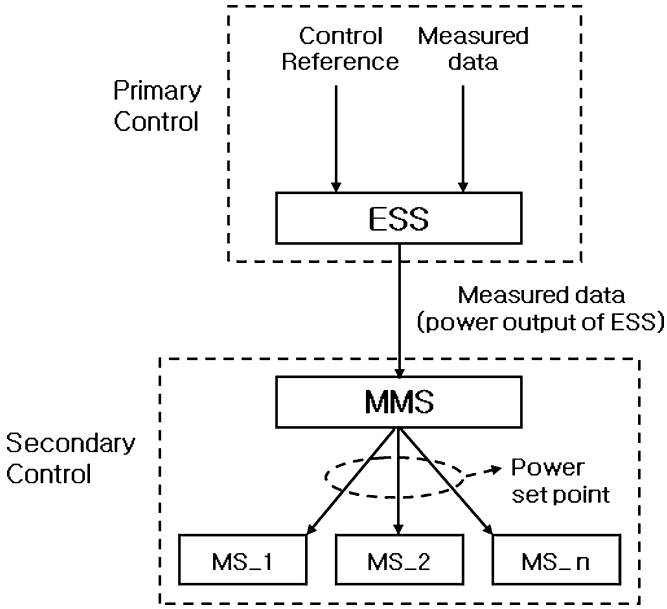

Fig. 10. Configuration of proposed cooperative control strategy.

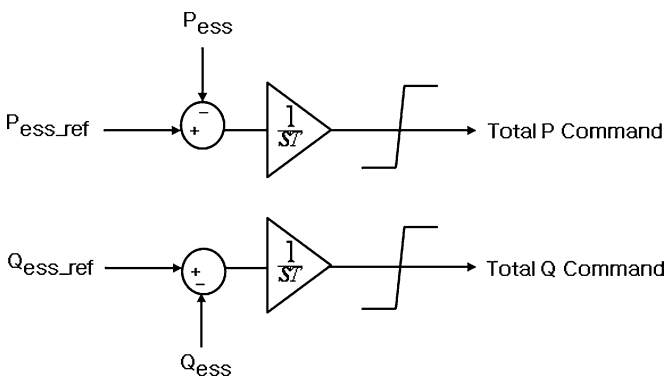

Fig. 11. Total power command generation.

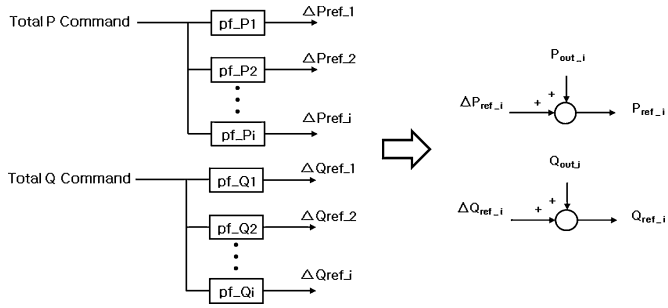

Fig. 12. Microsource power output set point calculation.

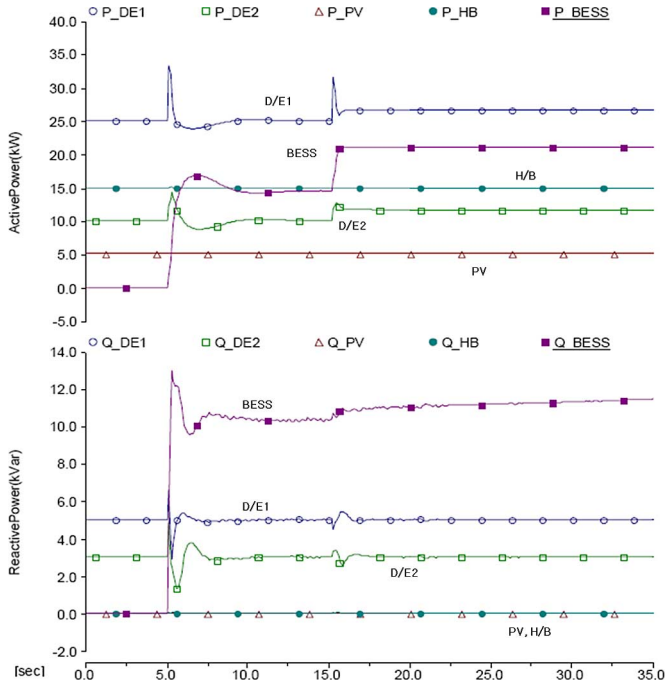

Fig. 13. (Case A) Power outputs of ESS and microsources.

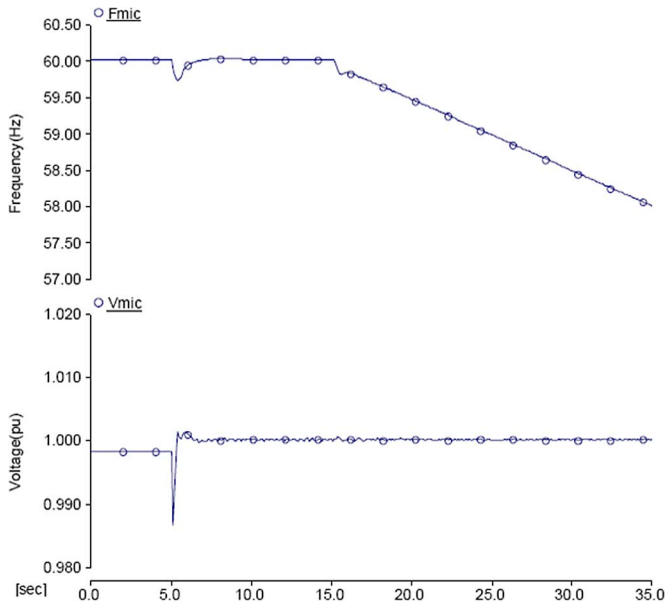

Fig. 14. (Case A) Frequency and voltage of microgrid.

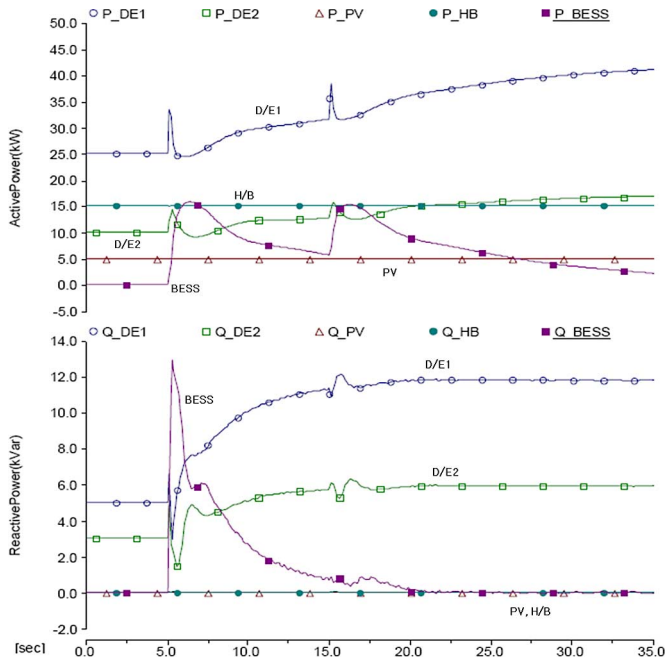

Fig. 15. (Case B) Power outputs of ESS and microsources.

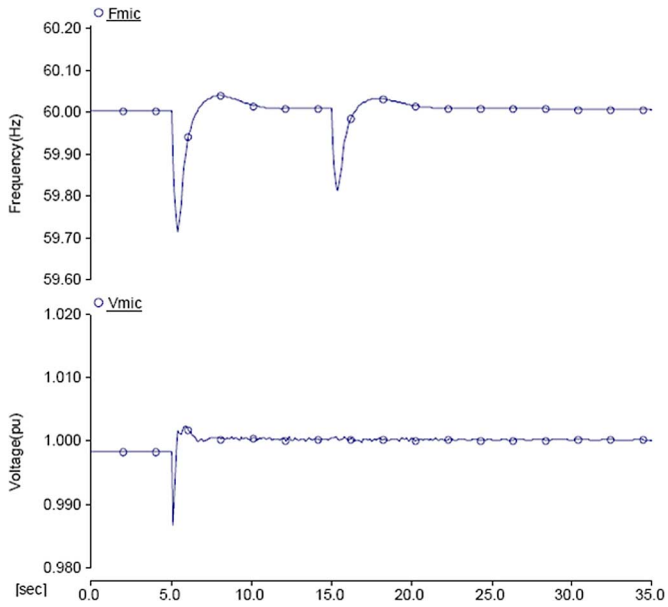

Fig. 16. (Case B) Frequency and voltage of microgrid.

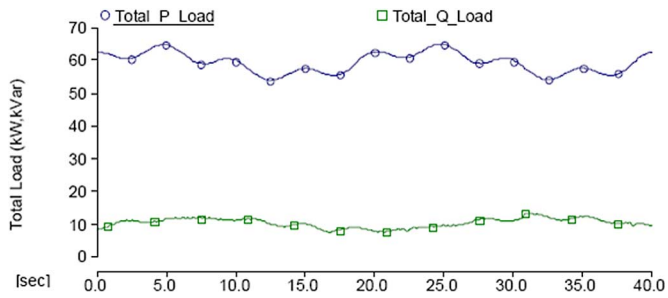

Fig. 17. (Case C) Load fluctuation during test period.

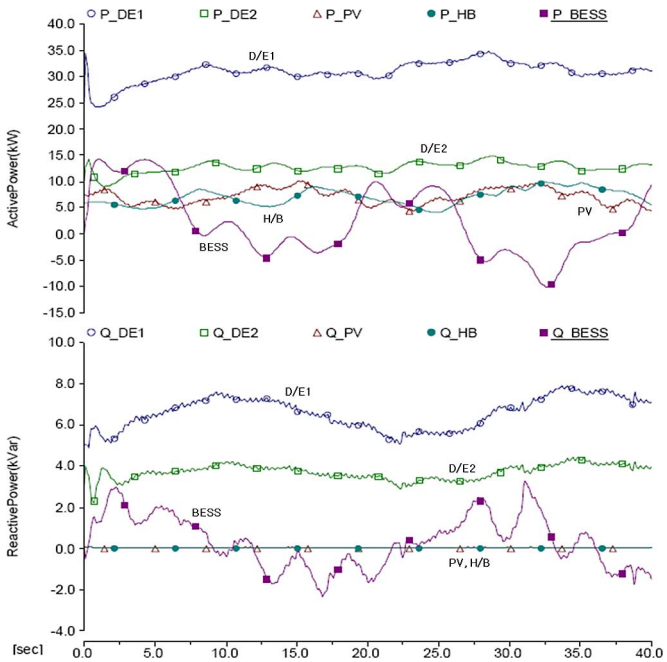

Fig. 18. (Case C) Power outputs of ESS and microsources.

utility grid when the fault occurs. The three loads are composed of linear RL branches, which can be changed automatically by remote load control device. The detailed aspects of test system are as follows:

1) test system configuration
   a) controllable source: Diesel generators
   b) renewable source: PV, PV, and WT Hybrid
   c) energy storage system: BESS
   d) Loads: Controllable constant impedance load (R/X)
2) generation capacity of microsources
   a) PV: 10 kW
   b) diesel generator: 70 kW (D/E1 50 kW, D/E2 20 kW)
   c) H/B: 20 kW (Wind 10 kW, PV 10 kW)
3) capacity of energy storage system
   a) BESS 10 kWh
   b) Power conditioning system of BESS system 20 kW
4) load
   a) load 1: 8 kW
   b) load 2: 80 kW+j32 kVar
   c) load 3: 12 kW+j12 kVar
5) transformer
   a) three phase 22.9/0.38 kV 100 kVA
   b) leakage impedance %Z = 6%
6) line impedance
   a) $R = 0.1878$ ohm/km, $X = 0.0968$ ohm/km.

IV. Control Strategy for Islanded Operation

A. Main Concept

The main concept for islanded operation involves the cooperative control of the ESS and other controllable microsources, as shown in Fig. 4. During islanding, the power balance between supply and demand does not match at the moment. As a result,

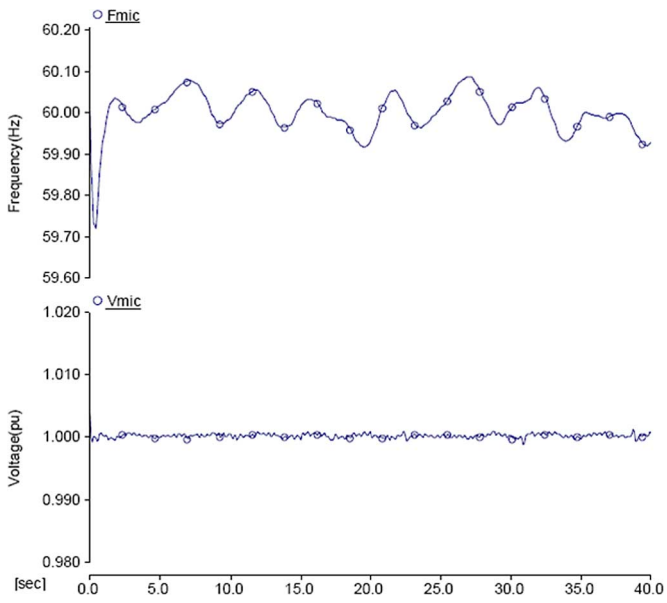

Fig. 19. (Case C) Frequency and voltage of microgrid.

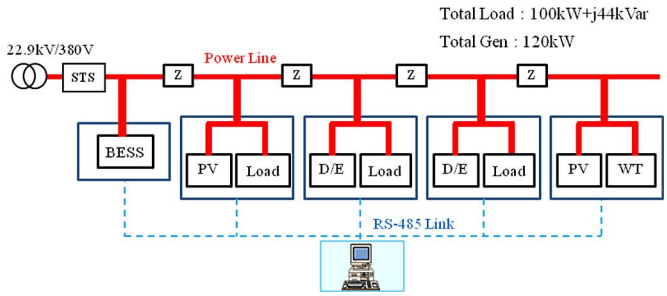

Fig. 20. Configuration of microgrid pilot plant.

the frequency and the voltage of the microgrid will fluctuate, and the system can experience a blackout unless there is an adequate power-balance matching process. The controller of inverter in the ESS responds in milliseconds. Otherwise, the diesel generator, gas engine, and fuel cell have a relatively slow response time. Obviously, the ESS should play an important role in maintaining the frequency and the voltage of the microgrid during islanded operation. In islanded operation, by proper power-balancing action of the ESS, the frequency and the voltage of the microgrid can be regulated at the normal values. However, the control capability of the ESS for balancing between generation and consumption may be limited by its available system capacity. Therefore, the power output of the ESS should be brought back to zero as soon as possible by the secondary control in MMS in order to secure the maximum spinning reserve.

B. Local Control of ESS

Fig. 5 shows the configuration of the BESS and its local controllers. The controller consists of upper grid operation controller and a d–q frame-based lower current controller [41]. In grid-connect operation, all of the microsources and the ESS are in PQ control mode, where the power output set point is provided by the MMS. In this mode, the upper controller regulates the active and the reactive power injected into the grid and outputs the d- and q-axis current commands, I_{d_ref} and I_{q_ref}. Otherwise, in islanded operation, the upper grid operation controller regulates the frequency and the voltage of microgrid, and also outputs the d- and q-axis current commands, as shown in Fig. 6. The transition from fixed power control to frequency and voltage is activated by information received from MMS. The MMS received the state of connection from STS and then the received information is passed to the BESS through serial communication link. The lower current control scheme is presented in Fig. 7. Once the current reference, I_{d_ref} and I_{q_ref}, is determined, d–q transformation control is applied to enable the active and reactive components of ac output power to be mutually independently controlled. In a current controller in Fig. 8, d- and q-axis reference voltage V_{d_ref} and V_{q_ref} are generated using errors between d–q current reference (I_{d_ref} and I_{q_ref}) and measured d–q current (I_d and I_q). The generated d–q reference voltage is transformed into the a-, b-, and c-axis reference voltage V_{a_ref}, V_{b_ref}, and V_{c_ref} by the d–q to abc transformation block. The phase-lock loop (PLL) block, as shown in Fig. 9, generates a signal synchronized in phase to the converter input voltage V_{abc} to provide the reference phase angle for the rotational inverse d–q transformation. When the desired voltages on the a–b–c frame are set, a pulse width modulation (PWM) technique is applied because of its simplicity and excellent performance. In the PWM block, the desired voltage waves $V_{\mathrm{abc\_ref}}$ and the triangular carrier signal are compared at crossover points and create turn-ON and turn-OFF switching signals for the six insulated gate bipolar transistors (IGBTs).

C. Secondary Control of MMS

In order to bring back the power output of the ESS to be zero, the MMS should calculate and dispatch the power output set point of each microsource through the secondary control function. The MMS can receive the information about system states by communication. The closed-loop control issues power output set point over the communication channel to each microsource. The LCs are ultimately responsible for regulating the power output locally in each component. Fig. 10 shows the feature of primary and secondary control action.

The secondary control algorithm in MMS compares the measured power output of BESS (P_{ess} and Q_{ess}) and the reference value ($P_{\mathrm{ess\_ref}}$ and $Q_{\mathrm{ess\_ref}}$) to obtain the error. This error generates the total required power (total P command and total Q command), as shown in Fig. 11. And generated commands are applied to the dispatch function which is presented by (1) and (2) to generate a power output set point for each individual controllable microsource

$$\Delta P_{\mathrm{ref}\_i} = p_{f\_P_i} . P_{\mathrm{total\_command}} \tag{1}$$

$$\Delta Q_{\mathrm{ref}\_i} = p_{f\_Q_i} . Q_{\mathrm{total\_command}} \tag{2}$$

where, $\Delta P_{\mathrm{ref}\_i}$ and $\Delta Q_{\mathrm{ref}\_i}$ is the variation of the power output set point for the ith microsource, and $p_{f\_P_i}$ and $p_{f\_Q_i}$ is the participant factor for the ith microsource. $P_{\mathrm{total\_command}}$ and $Q_{\mathrm{total\_command}}$ is total p and Q command generated by Fig. 11.

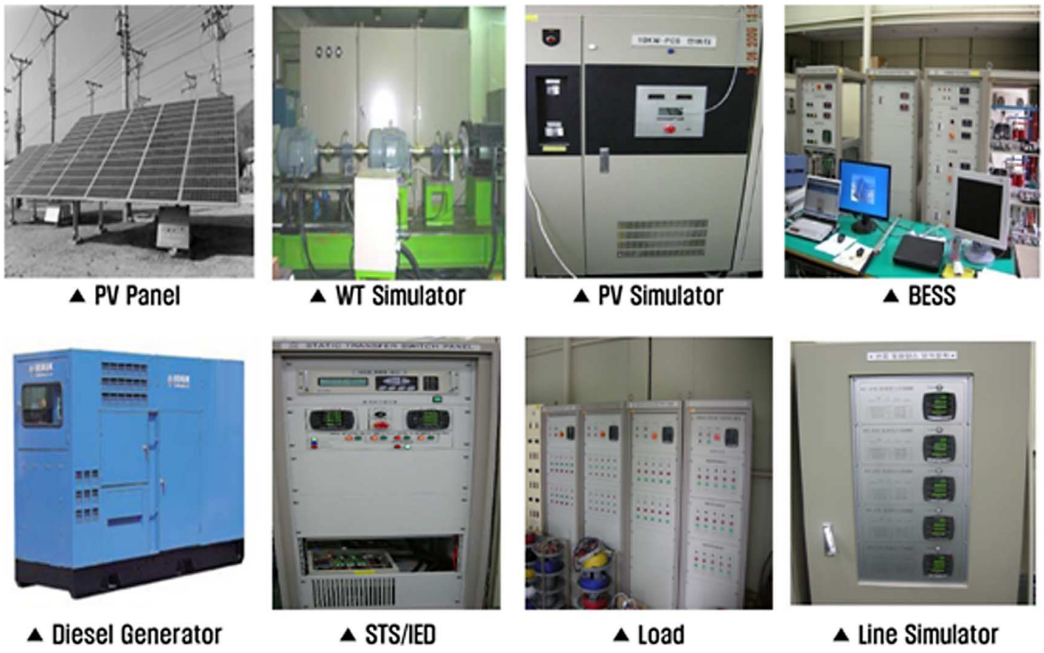

Fig. 21. Feature of the components in microgrid.

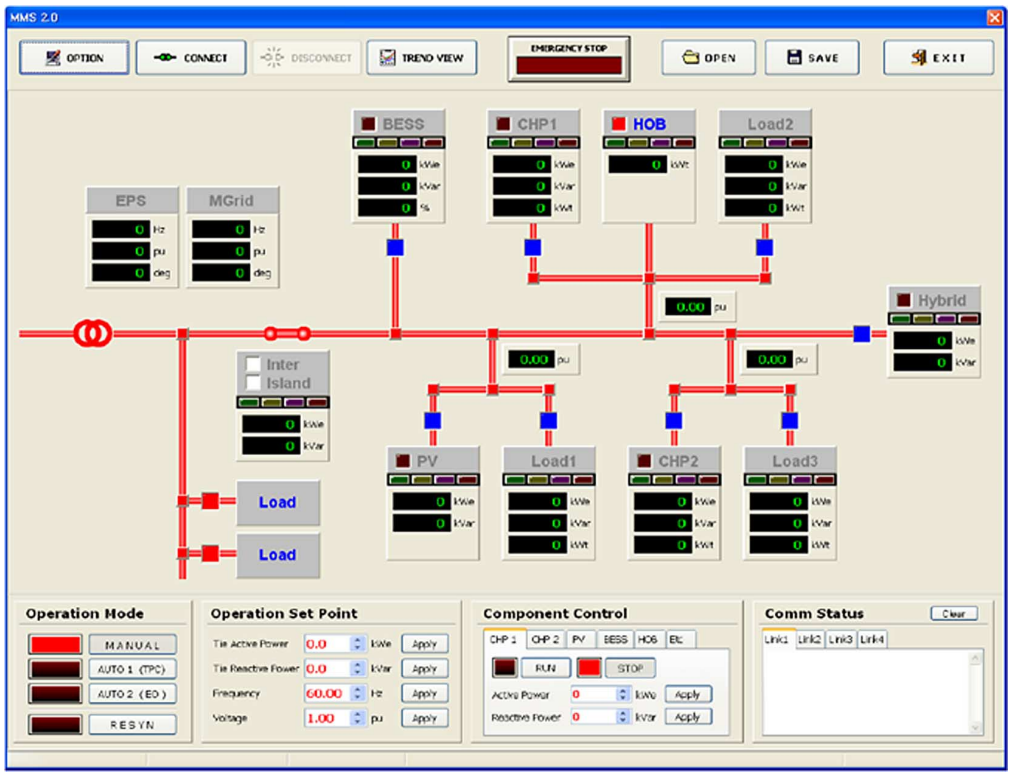

Fig. 22. Feature of developed MMS.

In (1) and (2), the participant factor of ith microsource is a predetermined constant value and it is decided by the capacity of the microsource. The final active power output set point of the ith microsource (P_{ref_i} and Q_{ref_i}) is determined by the summation of the current power output value (P_{out_i} and Q_{out_i}) and change of the power output set point ($\Delta P_{\mathrm{ref}\_i}$ and $\Delta Q_{\mathrm{ref}\_i}$), as shown in Fig. 12. This secondary control algorithm is executed every second by the MMS.

V. Simulation Study

A simulation platform under the PSCAD/EMTDC environment was developed to evaluate the dynamic behavior of the

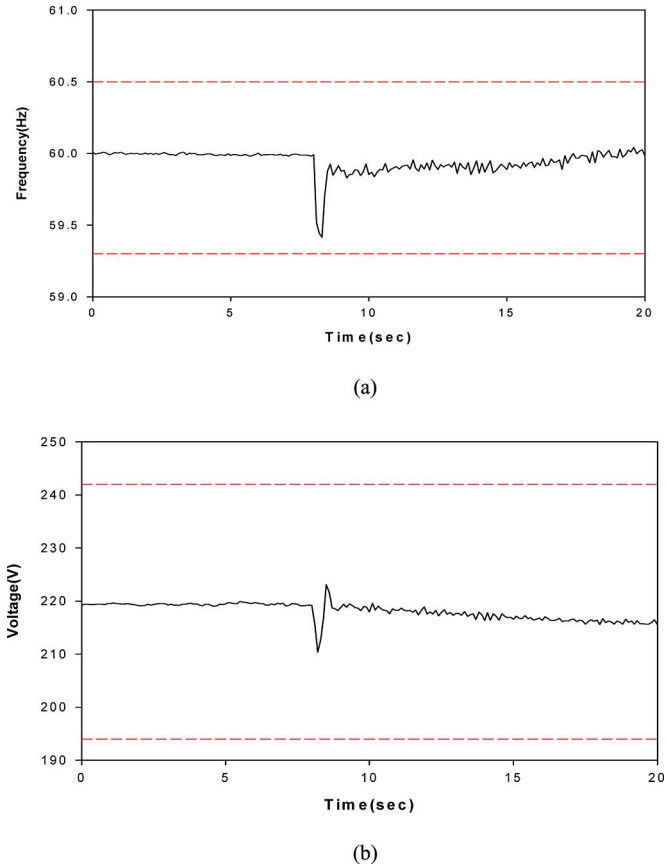

Fig. 23. Microgrid frequency and voltage when islanding operation is taking place at $t = 8$ s (without secondary control).

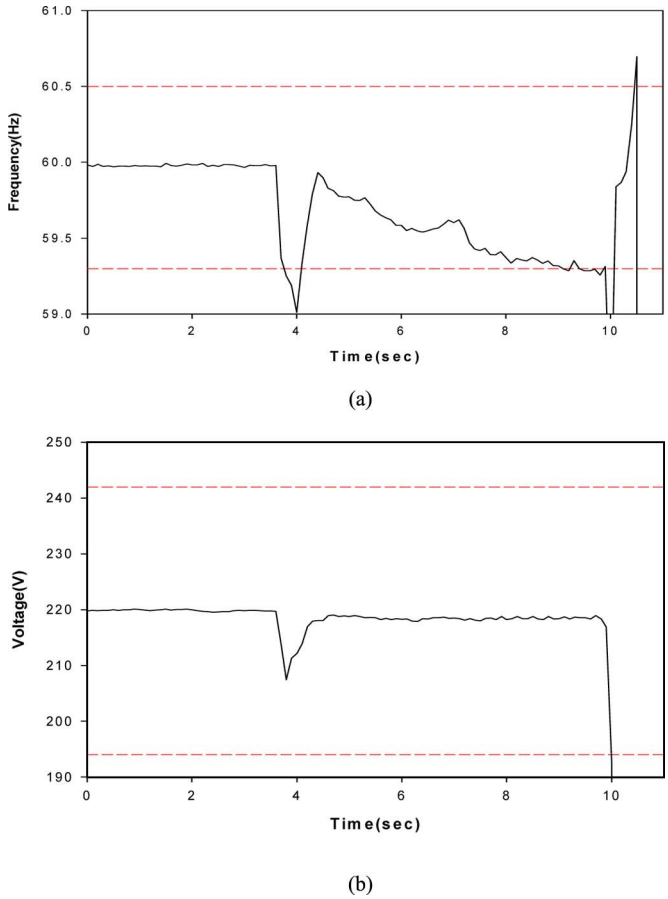

Fig. 24. Microgrid frequency and voltage when islanding operation is taking place at $t = 3.8$ s (without secondary control).

microgrid. In the PSCAD/EMTDC model, the RES and the BESS are modeled as an equivalent current source model for analysis convenience. A typical synchronous generator model in the PSCAD/EMTDC library is used to represent the diesel generators. The upstream grid is modeled by an equivalent voltage source with Thevenin impedance, and the load and line impedance are represented by constant impedance models, R and X.

Case A: Islanded operation without secondary control

In this case, the control mode of the BESS switches from fixed power control to frequency/voltage (F/V) control when the microgrid is disconnected from utility grid and the secondary control is not applied. The scenario is characterized by a total load of 70 kW + j17 kVar and the generation of PV 5 kW, H/B 15 kW, D/E1 25 kW + j5 kVar, and D/E2 10 kW + j3 kVar. The initial power output set point of the BESS in the grid-connect mode is set at zero. The two consecutive events are applied. A disconnect from utility grid occurs at $t = 5$ s and active load increases from 70 to 80 kW at $t = 15$ s. After islanding, the control scheme of the BESS shifts to F/V control. The power output of the BESS increases from zero to 17 kW + j11 kVar very quickly and settles down at 15 kW + j9 kvar, as shown in Fig. 13. Otherwise, the power outputs of microsources are maintained at an initial constant value. After a short transient period, the frequency and the voltage of the microgrid can maintain predefined normal values (60 Hz and 1.0 pu) due to the fast response of the BESS, as shown in Fig. 14. The power output of BESS in the steady state maintains a constant value after the first event. In the event of load change at $t = 15$ s followed by islanding, the ESS should inject the more of 10 kW of additional active power into the microgrid to make the balance. However, the ESS cannot support additional 10 kW of active power because it has only 5 kW of spinning reserve margin. This power unbalance makes the microgrid be unstable, as shown in Fig. 14.

Case B: Islanded operation with secondary control

In this case, the secondary control of the MMS is considered. The operating scenario is the same as the previous simulation case A. After islanding, the power output of BESS changes from zero to a certain value to control the frequency and the voltage as soon as the disturbance occurs, and then it is returned to zero due to secondary control action, which is performed in the MMS. During islanded operation, the power output of diesel generators are also changed from an initial constant value to a new power set point calculated by secondary control, as shown in Fig. 15. In the second event of 10 kW of active load change at $t = 15$ s, the ESS can afford to inject necessary active power into the microgrid to make power balance because the power output of the ESS is bringing back to zero and then it has enough spinning reserve margin. The power outputs of the diesel generators are

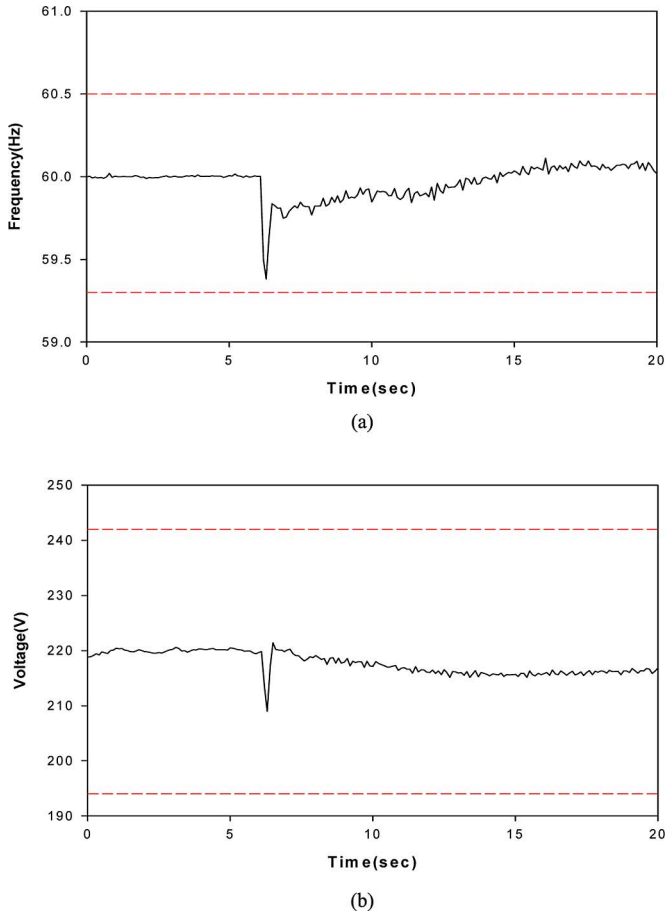

Fig. 25 Microgrid frequency and voltage when islanding operation is taking place at $t = 6.3$ s (with secondary control).

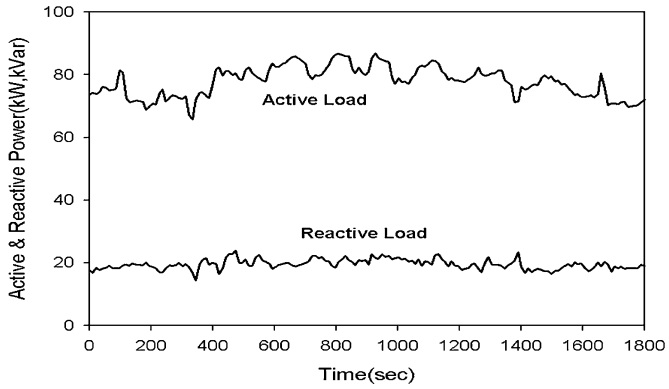

Fig. 26. Load fluctuation during test period.

changed from the initial constant values to new set points by MMS. By the help of this cooperative control, the frequency and the voltage can be regulated at nominal values successfully, as shown in Fig. 16.

Case C: Islanded operation with varying loads and RES power outputs

Finally, we evaluate the islanded operation performance of the microgrid under the condition of continuously varying loads and power outputs of RES. The islanding occurs at $t = 0$ s

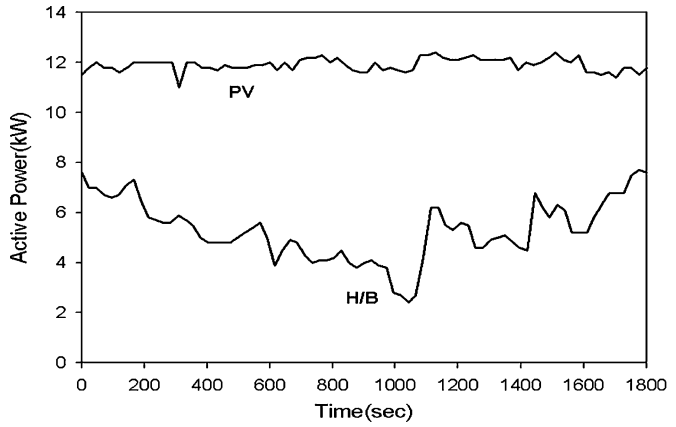

Fig. 27. Power outputs of H/B and PV.

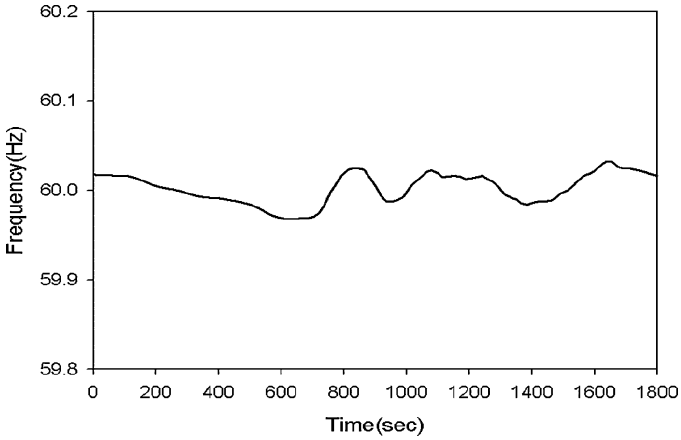

Fig. 28. Frequency of microgrid.

and loads and power output of the RES change, as shown in Figs. 17 and 18. According to the loads and power outputs of the RES change, the BESS injects or absorbs the power from the microgrid to regulate the frequency and the voltage. Then, the secondary control detects the changing in the power output of the BESS and assigns the new power output set point to the two diesel generators, as shown in Fig. 18. Through the cooperative control strategy, the microgrid can be operated in stable during islanded operation, as shown in Fig. 19.

VI. Experimental Study

A 120-kW microgrid pilot plant was developed. Figs. 20 and 21 show configuration and feature of microgrid pilot plant and each component. It is composed of a PV system, PV/wind hybrid system, BESS, diesel generators, STS, and loads. These components communicate with MMS software installed in a remote PC by RS485 serial communication. Fig. 22 shows the developed prototype MMS for management of microgrid pilot plant. System operation and supervisor control can be handled using MMS. It monitors and displays system current states including power outputs of microsources, voltage, frequency, state of charge of battery storage, and can also issue power output set points of microsources.

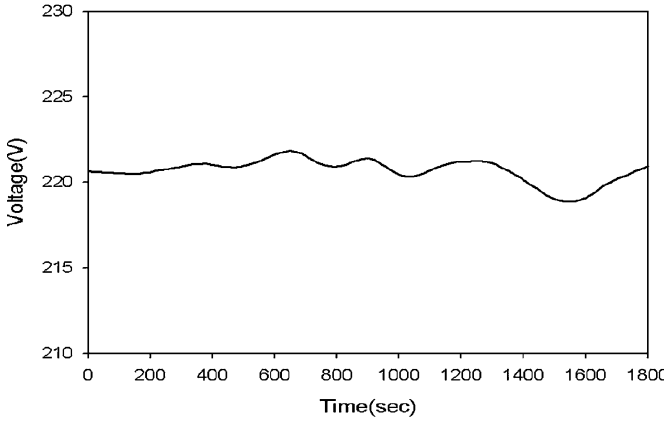

Fig. 29. Voltage of microgrid.

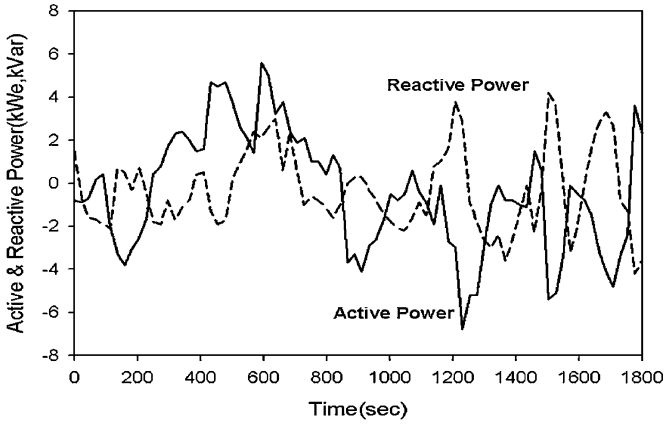

Fig. 30. Power output of BESS.

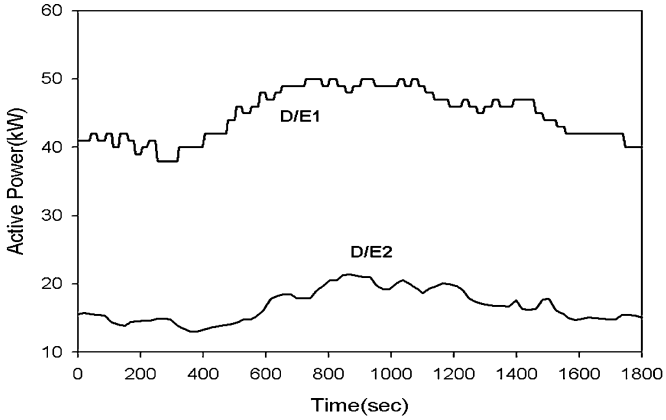

Fig. 31. Active power outputs of diesel engine generators.

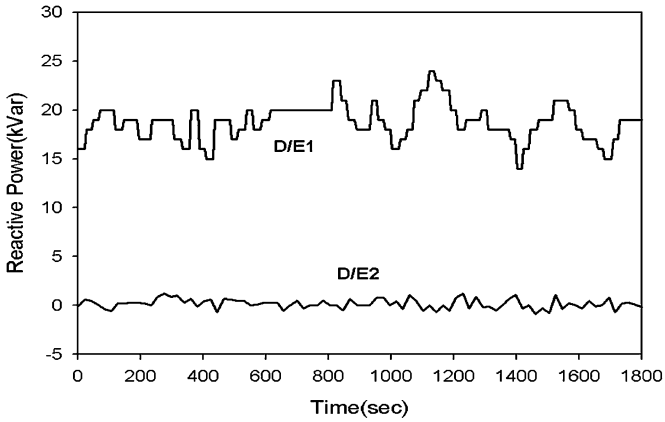

Fig. 32. Reactive power outputs of diesel engine generators.

In the first experiment case, the control performance in transit mode from grid-connect to islanded is evaluated by using pilot plant. Fig. 23 shows the experimental results with the initial condition of importing 15 kW + j0 kVar from utility grid. In this experiment, the secondary control action is not applied, and only the primary control action of the BESS is considered. The islanding occurs at $t = 8$ s, and the control scheme of the BESS shifts to F/V control. As shown in figures, the frequency and the voltage of microgrid can be maintained within the stable operation range, i.e., 59.3 to 60.5 Hz, 198 to 242 V. Fig. 24 shows the experimental results with the initial condition of importing 20 kW + j0 kVar from utility grid and the secondary control is also not applied. After islanding, the frequency and the voltage of the microgrid become unstable and finally system breaks down due to the limitation of maximum power output of the BESS. The protection function of the local controller in the BESS detects over current status and disconnects the BESS from the microgrid. On the other hand, the microgrid can operate in a stable way when the secondary control is applied. As shown in Fig. 25, the frequency and voltage can be maintained within the stable range. These experimental results indicate that the secondary control action can contribute to improve the system control performance. In this case, the secondary control prevents the BESS from overloading through the increasing the power outputs of diesel generators.

In the second experiment, the control performance of microgrid during the islanded mode with varying loads and power outputs of RES is evaluated. During the test period, the loads and power outputs of PV and H/B are varying in accordance with the time, as shown in Figs. 26 and 27. After islanding, the frequency of the microgrid maintains within the range from 59.8 to 60.2 Hz and the voltage also can be regulated from 0.9 to 1.1 pu, as shown in Figs. 28 and 29. The power output of BESS changes from zero to a certain value to control the frequency and the voltage, and it is returned to zero due to secondary control, as shown in Fig. 30.

During islanded operation, the power outputs of diesel engine generators are also changed from an initial constant value to a new set point, as shown in Figs. 31 and 32. The results show that the proposed cooperative control scheme can regulate the frequency and voltage very well.

VII. Conclusion

In this paper, the cooperative control strategy of the microsources and the ESS during islanded operation has been proposed. During islanding, the power balance between supply and demand does not match at the moment.

As a result, the frequency and voltage of the microgrid will fluctuate, and the system can experience a blackout unless there is an adequate power-balance matching process. The controller of inverter in the ESS responds in milliseconds. Otherwise, the diesel generator, gas engine, and fuel cell have a relatively slow response time. In islanded operation, by proper power-balancing action of the ESS, the frequency and the voltage of the microgrid can be regulated at the normal values. However, the control capability for balancing between generation and consumption of the ESS may be limited by its available system capacity. Therefore, the power output of the ESS should be brought back to zero as soon as possible by the secondary control in MMS in order to secure the maximum controlling reserve. Dynamic modeling and simulations of the microgrid under the proposed control strategy were carried out using PSCAD/EMTDC. A 120-kW microgrid pilot plant and its MMS was developed and tested. The results show that the proposed cooperative control scheme can regulate the frequency and the voltage very well. In addition, these results indicate that the secondary control action can contribute to improve the control capability.

REFERENCES

[1] N. Hatziargyriou, H. Asano, R. Iravani, and C. Marnay, "Microgrids," *IEEE Power Energy*, vol. 5, no. 4, pp. 78–94, Jul./Aug. 2007.

[2] N. Pogaku, M. Prodanovic, and T. C. Green, "Modeling, analysis and testing of autonomous operation of an inverter-based microgrid," *IEEE Trans. Power Electron.*, vol. 22, no. 2, pp. 613–625, Mar. 2007.

[3] J. M. Carrasco, L. G. Franquelo, J. T. Bialasiewiez, E. Galvan, R. C. P. Guisado, M. A. M. Prats, J. I. Leon, and N. Moreno-Alfonso, "Power-electronic systems for the grid integration of renewable energy sources: A survey," *IEEE Trans. Power Electron.*, vol. 53, no. 4, pp. 1002–1016, Aug. 2006.

[4] N. D. Hatziargyriou, "Microgrids," *IEEE Power Energy*, vol. 6, no. 3, pp. 26–29, May/Jun. 2008.

[5] G. Venkataramanan and C. Marnay, "A Larger role for microgrids," *IEEE Power Energy*, vol. 6, no. 3, pp. 78–82, May/Jun. 2008.

[6] C. Xiarnay, H. Asano, S. Papathanassiou, and G. Strbac, "Policymaking for microgrids," *IEEE Power Energy*, vol. 6, no. 3, pp. 66–77, May/Jun. 2008.

[7] A. Tsikalakis and N. Hatzargyriou, "Centralized control for optimizing microgrids operation," *IEEE Trans. Energy Convers.*, vol. 23, no. 1, pp. 241–248, Mar. 2008.

[8] S. Chakraborty, M. D. Weiss, and M. G. Simoes, "Distributed intelligent energy management system for a single-phase high-frequency AC microgrid," *IEEE Trans. Ind. Electron.*, vol. 54, no. 1, pp. 97–109, Feb. 2007.

[9] E. Barklund, N. Pogaku, M. Prodanovic, C. H. Aramburo, and T. C. Green, "Energy management in autonomous microgrid using stability-constrained droop control of inverters," *IEEE Trans. Power Electron.*, vol. 23, no. 5, pp. 2346–2352, Sep. 2008.

[10] T. Kinoshita and H. M. Kim, "A multiagent system for microgrid operation in the grid-interconnected mode," *J. Electr. Eng. Technol.*, vol. 5, no. 2, pp. 246–254, Jun. 2010.

[11] K. De Brabandere, B. Bolsens, J. Van den Keybus, A. Woyte, J. Driesen, and R. Belmans, "A voltage and frequency droop control method for parallel inverters," *IEEE Trans. Power Electron.*, vol. 22, no. 4, pp. 1107–1115, Jul. 2007.

[12] C. K. Sao and P. W. Lehn, "Control and power management of converter fed microgrids," *IEEE Trans. Power Syst.*, vol. 23, no. 3, pp. 1088–1098, Aug. 2008.

[13] J. M. Guerrero, J. Matas, L. G. Vicuna, M. Castilla, and J. Miret, "Decentralized control for parallel operation of distributed generation inverters using resistive output impedance," *IEEE Trans. Ind. Electron.*, vol. 54, no. 2, pp. 994–1004, Apr. 2007.

[14] J. M. Guerrero, J. C. Vasquez, J. Matas, M. Castilla, and L. G. de Vicuna, "Control strategy for flexible microgrid based on parallel line-interactive UPS systems," *IEEE Trans. Ind. Electron.*, vol. 56, no. 3, pp. 726–736, Mar. 2009.

[15] J. M. Guerrero, J. Matas, L. G. De Vicuna, M. Castilla, and J. Miret, "Wireless-control strategy for parallel operation of distributed-generation inverters," *IEEE Trans. Ind. Electron.*, vol. 53, no. 5, pp. 1461–1470, Oct. 2006.

[16] R. Majumder, A. Ghosh, G. Ledwich, and F. Zare, "Power management and power flow control with back-to-back converters in a utility connected microgrid," *IEEE Trans. Power Syst.*, vol. 25, no. 2, pp. 821–834, May 2010.

[17] C. L Chen, Y. W. Wang, J. S. Lai, Y. S. Lee, and D. Martin, "Design of parallel inverters for smooth mode transfer microgrid applications," *IEEE Trans. Power Electron.*, vol. 25, no. 1, pp. 6–15, Jan. 2010.

[18] G. Diaz, C. Gonzalez-Moran, J. Gomez-Aleixandre, and A. Diez, "Scheduling of droop coefficients for frequency and voltage regulation in isolated microgrids," *IEEE Trans. Power Syst*, vol. 25, no. 1, pp. 489–496, Feb. 2010.

[19] H. L. Jou, W. J. Chiang, and J. C. Wu, "A simplified control method for the grid-connected inverter with the function of islanding detection," *IEEE Trans. Power Electron.*, vol. 23, no. 6, pp. 2775–2783, Nov. 2008.

[20] D. M. Vilathgamuwa, P. C. Loh, and Y. Li, "Protection of microgrids during utility voltage sags," *IEEE Trans. Ind. Electron.*, vol. 53, no. 5, pp. 1427–1436, Oct. 2006.

[21] J. Stevens, H. Vollkommer, and D. Klapp, "CERTS microgrid system tests," in *Proc. IEEE Power Eng. Soc. Gen. Meet.*, Jun., 2007, pp. 1–4.

[22] B. Kroposki, R. Lasseter, T. Ise, S. Morozumi, S. Papatlianassiou, and N. Hatziargyriou, "Making microgrids work," *IEEE Power Energy*, vol. 6, no. 3, pp. 40–53, May/Jun. 2008.

[23] C. Marnay, G. Venkataramanan, M. Stadler, A. S. Siddiqui, R. Firestone, and B. Chandran, "Optimal technology selection and operation of commercial-building microgrids," *IEEE Trans. Power Syst.*, vol. 23, no. 3, pp. 975–982, Aug. 2008.

[24] A. Amorim, A. L. Cardoso, J. Oyarzabal, and N. Melo, "Analysis of the connection of a microturbine to a low voltage grid," presented at the Int. Conf. Future Power Syst., 16–18 Nov., 2005, Amsterdam, Netherlands.

[25] A. K. Saha, S. Chowdhury, S. P. Chowdhury, and P. A. Crossley, "Modeling and performance analysis of a microturbine as a distributed energy resource," *IEEE Trans. Energy Convers.*, vol. 24, no. 2, pp. 529–538, Jun. 2009.

[26] EU Microgrid Project, "Microgrids large scale integration of microgeneration to low voltage grids", ENK-5-CT-2002–00610, 2004.

[27] L. Zbiniew and W. B. Janusz, "Supervisory control of a wind farm," *IEEE Trans. Power Syst.*, vol. 22, no. 3, pp. 985–994, Aug. 2007.

[28] S. Teleke, M. E. Baran, A. Q. Huang, S. Bhattacharya, and L. Anderson, "Control strategies for battery energy storage for wind farm dispatching," *IEEE Trans. Energy Convers.*, vol. 24, no. 3, pp. 725–732, Sep. 2009.

[29] C. Abbey and G. Joos, "Supercapacitor energy storage for wind energy applications," *IEEE Trans. Ind. Appl.*, vol. 43, no. 3, pp. 769–776, May/Jun. 2007.

[30] M. Pascal, C. Rachid, and O. Alexandre, "Optimizing a battery energy storage system for frequency control application in an isolated power system," *IEEE Trans. Power Syst.*, vol. 24, no. 3, pp. 1469–1477, Aug. 2009.

[31] S. C. Tripathy, M. Kalantar, and R. Balasubramanian, "Dynamic and stability of wind and diesel turbine generators with superconducting magnetic energy storage unit on an isolated power system," *IEEE Trans. Energy Convers.*, vol. 6, no. 4, pp. 579–585, Dec. 1991.

[32] A. R. Kim, H. R. Seo, G. H. Kim, M. W. Park, I. K. Yu, Y. Otsuki, J. Tamura, S. H. Kim, K. D. Sim, and K. C. Seong, "Operating characteristic analysis of HTS SMES for frequency stabilization of dispersed power generation system," *IEEE Trans. Appl. Supercond.*, vol. 20, no. 3, pp. 1334–1338, Jun. 2010.

[33] P. Thounthong, S. Rael, and B. Davat, "Analysis of supercapacitor as second source based on fuel cell power generation," *IEEE Trans. Energy Convers.*, vol. 24, no. 1, pp. 247–255, Mar. 2009.

[34] L. Yunwei, D. Mahinda, V. Poh, and L. Chiang, "Design, analysis, and real-time testing of a controller for multibus microgrid system," *IEEE Trans. Power Electron.*, vol. 19, no. 5, pp. 1195–1204, Sept. 2004.

[35] Y. W. Li and C. N. Kao, "An accurate power control strategy for power-electronics-interfaced distributed generation units operating in a low-voltage multibus microgrid," *IEEE Trans. Power Electron.*, vol. 24, no. 12, pp. 2977–2988, Dec. 2009.

[36] T. Tanabe, S. Suzuki, Y. Ueda, T. Ito, S. Numata, E. Shimoda, T. Funabashi, and R. Yokoyama, "Control performance verification of power system stabilizer with an EDLC in islanded microgrid," *IEEJ Trans. Power and Energy*, vol. 129, no. 1, pp. 139–147, 2009.

[37] J. A. P. Lopes, C. L. Moreira, and A. G. Madureira, "Defining control strategies for microgrids islanded operation," *IEEE Trans. Power Syst.*, vol. 21, no. 2, pp. 916–924, May 2006.
[38] P. Kundur, "Power system stability and control," McGraw-Hill, NY, 1994.
[39] P. Paolo and L. Robert, "Autonomous control of microgrids," *IEEE Power Eng. Soc. Meeting*, Montreal, Canada, Jun. 18–22, 2006.
[40] F. Katiraei, R. Iravani, N. Hatziargyriou, and A. Dimeas, "Microgrids management-controls and operation aspects of microgrids," *IEEE Power Energy*, vol. 6, no. 3, pp. 54–65, May/Jun. 2008.
[41] A. Timbus, M. Liserre, R. Teodorescu, P. Rodriguez, and F. Blaabjerg, "Evaluation of current controllers for distributed power generation systems," *IEEE Trans. Power Electron.*, vol. 24, no. 3, pp. 654–664, Mar. 2009.

Jong-Yul Kim (M'09) received the B.S. and M.S. degrees in electrical engineering from Pusan National University, Busan, Korea.

Since 2001, he has been with the Korea Electrotechnology Research Institute (KERI), Changwon, Korea. He is currently a Senior Research Engineer at the New & Renewable Energy System Research Center, KERI. His research interests include power system analysis, and design and operation of microgrid and smart grid.

Jin-Hong Jeon (M'09) received the B.S. and M.S. degrees in electrical engineering from Sungkyunkwan University, Suwon, Korea.

He is currently a Senior Research Engineer at the New & Renewable Energy System Research Center, Korea Electrotechnology Research Institute, Changwon, Korea. His research interests include the design of control algorithm and the implementation of power conversion systems in the fields of flexible AC transmission system (FACTS), and microgrid with renewable energy resources.

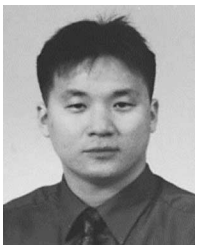

Seul-Ki Kim (M'09) received the B.S., M.S., and Ph.D. degrees in electrical engineering from Korea University, Seoul, Korea, in 1998, 2000, and 2010, respectively.

Since 2000, he has been with Korea Electrotechnology Research Institute, Changwon, Korea, where he is currently a Senior Research Engineer at the New & Renewable Energy System Research Center. His research interests include grid interface of distributed generators, and modeling and analysis of distributed generation resources.

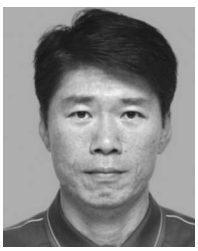

Changhee Cho (M'09) received the B.S. and M.S. degrees in electrical engineering from Seoul National University, Seoul, Korea.

He is currently a Senior Researcher at the New & Renewable Energy System Research Center, Korea Electrotechnology Research Institute, Changwon, Korea. His research interests include control and management of the dispersed energy resources, network communication, and energy optimization of microgrids.

June Ho Park received the B.S., M.S. and Ph.D. degrees from Seoul National University, Seoul, Korea in 1978, 1980, and 1987, respectively, all in electrical engineering.

He is currently a Professor at the School of Electrical Engineering, Pusan National University, Busan, Korea. His research interests include intelligent systems applications to power systems.

Dr. Park has been a member of the IEEE POWER ENGINEERING SOCIETY.

Hak-Man Kim (M'09) received the B.S., M.S. and Ph.D. degrees in electrical engineering from Sungkyunkwan University, Korea, in 1991, 1993, and 1998, respectively.

From October 1996 to February 2008, he was a Senior Researcher at Korea Electrotechnology Research Institute, Changwon, Korea. He is currently a Professor at the Department of Electrical Engineering, University of Incheon, Incheon, Korea. His research interests include power system analysis, agent-based autonomous power grids, and artificial intelligent applications in power system engineering.

Dr. Kim is a senior member of the Korean Institute of Electrical Engineers and the Institute of Electrical, Information and Communication Engineers, Japan.

.

Kee-Young Nam received the B.S. and M.S. degrees from the Department of Electrical Engineering, Sungkyunkwan University, Seoul, Korea, in 1982 and 1984, respectively, and the Ph.D. degree from Ibaraki University, Hitachi, Japan, in 1998.

From 1984 to 2009, he was a Principal Researcher at the Power System Division, Korea Electrotechnology Research Institute, Changwon, Korea. He is currently the Head of Research and Development Center, Halla Energy & Environment Company, Seoul, Korea. His research interests include optimization of operating distribution system and automation, power quality analysis and diagnosis, renewable energy system, and micro- and smart grid system design and operation.